

# Far-Field Pattern Reconstruction from a Nonredundant Plane-Polar Near-Field Sampling Arrangement: Experimental Testing

F. D'Agostino, F. Ferrara, C. Gennarelli, *Senior Member, IEEE*, R. Guerriero, M. Migliozzi

**Abstract**— An efficient probe-compensated near-field – far-field (NF–FF) transformation with plane-polar scanning, particularly suitable for quasi-planar antennas, is experimentally assessed in this letter. It exploits the nonredundant sampling representations of electromagnetic fields and adopts an oblate ellipsoid to model the antenna under test. A two-dimensional optimal sampling interpolation expansion is employed to accurately recover the NF data needed by the standard plane-rectangular NF–FF transformation from the nonredundant plane-polar ones collected by the probe. A remarkable reduction of the number of NF data to be acquired and of the related measurement time is so obtainable. Some results of the experimental tests, performed at the UNISA Antenna Characterization Lab and assessing the effectiveness of such a NF–FF transformation technique, are reported.

**Index Terms**—Antenna measurements, nonredundant sampling representations of electromagnetic fields, plane-polar near-field – far-field transformation.

## I. INTRODUCTION

As well-known the near-field – far-field (NF–FF) transformations [1], [2] are well-assessed and widely used techniques for the precise determination of the radiation pattern of electrically large antennas from NF measurements performed in an anechoic chamber and allow one to overcome the drawbacks of direct measurements in a conventional FF range. Among the NF–FF transformations, the classical plane-rectangular one [3], [4] is particularly suitable for highly directive antennas characterized by pencil beam patterns well within the solid angle specified by the edges of the antenna under test (AUT) and those of the scanning area. The NF–FF transformation with plane-polar scanning (see Fig. 1) is a convenient and appealing alternative to the classical one. In fact, the plane-polar scanning is from a mechanical viewpoint simpler than the plane-rectangular one, because it can be done by rotating the AUT while moving the probe linearly. Moreover, for a given size of the anechoic chamber, it allows one to cover a scanning area greater than in the plane-rectangular case. The drawback of the earliest approach [5], namely, the very large computer time needed to reconstruct the antenna far field, has been overcome in [6] by applying the bivariate Lagrange interpolation to

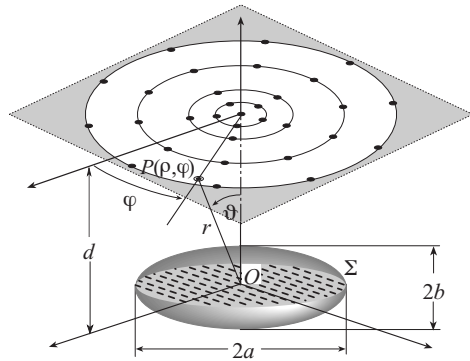


Fig. 1. Plane-polar scanning for a quasi-planar antenna.

recover the plane-rectangular data from the plane-polar ones, thus enabling the use of the FFT algorithm for the FF evaluation. However, such a simple technique is not particularly suitable to interpolate antenna radiated fields, so that it requires very close NF data spacings to make the interpolation error negligible. A more efficient interpolation scheme, relying on the spatial quasi-bandlimitation properties of radiated electromagnetic (EM) fields [7] and using the optimal sampling interpolation (OSI) expansions of central type, has been proposed in [8]. Although the number of data required by the technique in [8] is remarkably lower than in [5], [6], and [9], such a number is still unbounded when the size of the scanning zone approaches infinity. At last, by exploiting the nonredundant sampling representations of the EM fields [10], [11] and assuming the antenna as enclosed in a double bowl or in an oblate ellipsoid, efficient sampling representations over a plane from a minimum number of plane-polar samples (which stays finite also for an unbounded scanning plane) have been developed in [12] and [13], respectively. A remarkable saving of the number of the needed NF data and related measurement time is so obtained in the case of large antennas and extended scanning zones. This is a very important result, since the measurement time is nowadays even many orders of magnitude greater than the computer time to carry out the NF–FF transformation.

Aim of this paper is to provide the experimental assessment of the NF–FF transformation with plane-polar scanning [13], which uses an oblate ellipsoid to model a quasi-planar AUT. Such a model reduces the redundancy of the spherical one for these antennas and allows the use of measurement planes at distances less than one half of the AUT maximum size, thus lowering the error due to the truncation of the scanning surface.

Manuscript received September 16, 2015.

The authors are with the Department of Industrial Engineering, University of Salerno, 84084 Fisciano (SA), Italy (e-mail: cgennarelli@unisa.it).

## II. NONREDUNDANT VOLTAGE REPRESENTATION

Let us consider a quasi-planar AUT, enclosed in an oblate ellipsoid  $\Sigma$  with major and minor semi-axes equal to  $a$  and  $b$ , and a nondirective probe scanning a plane at distance  $d$  from the AUT center via a plane-polar NF facility system (Fig. 1). The spherical coordinate system  $(r, \vartheta, \phi)$  is adopted to denote any observation point, whereas a point  $P$  lying on the plane can be also identified by the plane-polar coordinates  $(\rho, \phi)$ . Since the voltage measured by a nondirective probe is a spatially quasi-bandlimited function having the same effective spatial bandwidth of the AUT field [14], the nonredundant sampling representations of EM fields [10], [11] can be exploited to obtain an efficient voltage representation requiring a minimum number of samples. Therefore, it is convenient to introduce the “reduced voltage”

$$\tilde{V}(\xi) = V(\xi) e^{j\gamma(\xi)} \quad (1)$$

where  $V(\xi)$  is the voltage  $V_\phi$  or  $V_\rho$  measured by the probe or by the rotated probe,  $\xi$  is the optimal parameter used to describe the curves (radial lines and rings) representing the plane in a plane-polar reference system, and  $\gamma(\xi)$  is a proper phase function. Since  $\tilde{V}(\xi)$  is not rigorously spatially bandlimited, an error occurs when approximating it with a bandlimited function. In any case, such a bandlimitation error is negligible as the bandwidth exceeds a critical value  $W_\xi$  [10] and can be effectively controlled by considering a bandwidth equal to  $\chi' W_\xi$ , where  $\chi'$  is a bandwidth enlargement factor slightly greater than unity for electrically large antennas [7].

For a radial line, it results [10], [13]:

$$W_\xi = (4a/\lambda) E(\pi/2|\varepsilon^2) \quad (2)$$

$$\xi = (\pi/2) [E(\sin^{-1} u |\varepsilon^2) / E(\pi/2 |\varepsilon^2)] \quad (3)$$

$$\gamma = \beta a \left[ v \sqrt{\frac{v^2 - 1}{v^2 - \varepsilon^2}} - E \left( \cos^{-1} \sqrt{\frac{1 - \varepsilon^2}{v^2 - \varepsilon^2}} | \varepsilon^2 \right) \right] \quad (4)$$

where  $\lambda$  is the wavelength,  $E(\cdot | \cdot)$  is the elliptic integral of second kind,  $\beta$  is the wavenumber,  $u = (r_1 - r_2)/2f$  and  $v = (r_1 + r_2)/2a$  are the elliptic coordinates,  $r_{1,2}$  being the distances from the point  $P$  to the foci of  $C'$  (intersection ellipse between a meridian plane and  $\Sigma$ ),  $2f$  the focal distance, and  $\varepsilon = f/a$  the eccentricity.

On a ring,  $\gamma$  is constant and any parameter proportional to the curvilinear abscissa is optimal, therefore it is convenient to choose  $\varphi$  as optimal parameter [10]. The related bandwidth is  $W_\varphi(\xi) = \beta a \sin \vartheta_\infty(\xi)$ , where  $\vartheta_\infty = \sin^{-1} u$  [10], [13].

The reduced voltage at the point  $P$  on the radial line specified by  $\varphi$  can be reconstructed via the OSI expansion [10], [13]:

$$\tilde{V}(\xi(\varphi), \varphi) = \sum_{n=n_0-q+1}^{n_0+q} \tilde{V}(\xi_n, \varphi) G(\xi, \xi_n, \bar{\xi}, N, N') \quad (5)$$

wherein  $2q$  is the number of retained intermediate samples  $\tilde{V}(\xi_n, \varphi)$ , i.e., the reduced voltages at the intersection points between the radial line through  $P$  and the sampling parallels,  $n_0 = \lfloor \xi / \Delta \xi \rfloor$ ,

$$\xi_n = n \Delta \xi = 2\pi n / (2N'' + 1); \quad N'' = \lfloor \chi N' \rfloor + 1 \quad (6)$$

$$N' = \lfloor \chi' W_\xi \rfloor + 1; \quad N = N'' - N'; \quad \bar{\xi} = q \Delta \xi \quad (7)$$

$\lfloor x \rfloor$  is the integer part of  $x$ ,  $\chi > 1$  an oversampling factor needed to control the truncation error [10], and

$$G(\xi, \xi_n, \bar{\xi}, N, N') = \Omega_N(\xi - \xi_n, \bar{\xi}) D_{N''}(\xi - \xi_n) \quad (8)$$

is the OSI interpolation function. Moreover,

$$D_{N''}(\xi) = \frac{\sin[(2N''+1)\xi/2]}{(2N''+1) \sin(\xi/2)} \quad (9)$$

$$\Omega_N(\xi, \bar{\xi}) = \frac{T_N[2\cos^2(\xi/2)/\cos^2(\bar{\xi}/2) - 1]}{T_N[2/\cos^2(\bar{\xi}/2) - 1]} \quad (10)$$

are the Dirichlet and Tschebyscheff sampling functions [10],  $T_N(\xi)$  being the Tschebyscheff polynomial of degree  $N$ .

The intermediate samples are recovered by interpolating the samples acquired on the rings via a quite similar OSI expansion along as  $\varphi$  [13]. The two-dimensional expansion to recover the voltage at any point on the plane is then determined [13] by matching the one-dimensional ones, thus obtaining:

$$V(\xi(\vartheta), \varphi) = e^{-j\gamma(\xi)} \sum_{n=n_0-q+1}^{n_0+q} \left\{ G(\xi, \xi_n, \bar{\xi}, N, N') \cdot \sum_{m=m_0-p+1}^{m_0+p} \tilde{V}(\xi_n, \varphi_m, n) G(\varphi, \varphi_m, \bar{\varphi}, M_n, M'_n) \right\} \quad (11)$$

where  $m_0 = \lfloor \varphi / \Delta \varphi_n \rfloor$ ,  $2p$  is the retained samples number along  $\varphi$ ,

$$\varphi_{m,n} = m \Delta \varphi_n = 2\pi m / (2M'_n + 1); \quad M'_n = \lfloor \chi M'_n \rfloor + 1 \quad (12)$$

$$M'_n = \lfloor \chi^* W_\varphi(\xi_n) \rfloor + 1; \quad M_n = M'' - M'_n; \quad \bar{\varphi} = p \Delta \varphi_n \quad (13)$$

$$\chi^* = 1 + (\chi' - 1) [\sin \vartheta_\infty(\xi_n)]^{-2/3} \quad (14)$$

and the other symbols have the same meanings as in (5). Note that the variation of  $\chi^*$  with  $\xi$  is required to guarantee a bandlimitation error constant on each sampling ring.

By applying (11), it is possible to reconstruct in an accurate and efficient way the voltages  $V_\phi$  and  $V_\rho$ , which would be acquired by the probe and rotated probe, at the points needed by the standard plane-rectangular NF-FF transformation [3], [4]. Unfortunately, the probe corrected formulas in [4] (whose expressions in the here used reference system are reported in [15]) are valid when the probe maintains its orientation with respect to the AUT and this requires its co-rotation with it. In any case, such a co-rotation can be avoided by using a probe exhibiting only a first-order azimuthal dependence in its radiated far field, as, e.g., an open-ended rectangular waveguide excited by a TE<sub>10</sub> mode [16]. In fact, in such a case, the voltages  $V_V$  and  $V_H$  (measured by the probe and rotated probe with co-rotation) can be determined from  $V_\phi$  and  $V_\rho$  via the relations:

$$V_V = V_\phi \cos \varphi - V_\rho \sin \varphi; \quad V_H = V_\phi \sin \varphi + V_\rho \cos \varphi \quad (15)$$

### III. EXPERIMENTAL ASSESSMENT

The tests assessing the effectiveness of the described technique have been performed on two different antennas in the anechoic chamber of the UNISA Antenna Characterization Lab, equipped with a plane-polar NF facility, besides the cylindrical and spherical ones. The plane-polar scanning is performed by mounting the AUT on a roll positioner and the probe (an open-ended WR90 rectangular waveguide) on a vertical scanner.

The AUT considered in the first set of figures is a X-band flat plate slot array of Rantec Microwave Systems Inc., with radius of 23 cm, located on the plane  $z = 0$  and working at 9.3 GHz. It has been enclosed within an oblate ellipsoid with  $a = 23.5$  cm, and  $b = 9.0$  cm. The NF data have been acquired in a circle with radius 110 cm on a plane at  $z = 18.3$  cm. The amplitude and phase of  $V_\rho$  on the radial line at  $\varphi = 0^\circ$ , recovered from the nonredundant plane-polar NF data, are compared in Figs. 2 and 3 with those directly measured on the same line. The comparison between the recovered amplitudes of  $V_\rho$  and  $V_\varphi$  on the radial line at  $\varphi = 30^\circ$  and the directly measured ones is also shown in Fig. 4. As can be seen, all reconstructions are very accurate, save for small differences occurring in the peripheral zones characterized by very low voltage levels. Note that the low pass filtering properties of the interpolation functions allow to cut away the spatial harmonics of the noise outside the AUT spatial bandwidth, so that the interpolated voltages exhibit a smoother behaviour with respect to the directly measured ones. The overall effectiveness of this technique is assessed by comparing the recovered FF patterns in

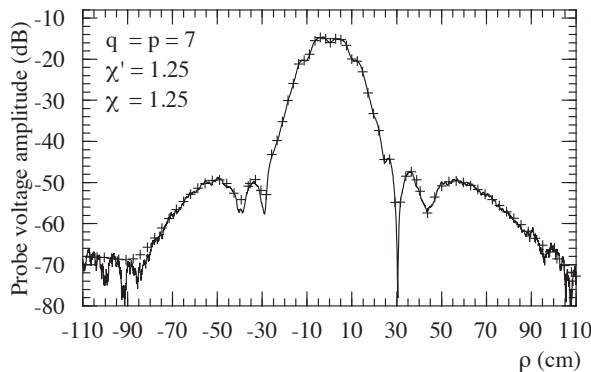


Fig. 2. Amplitude of  $V_\rho$  on the radial line at  $\varphi = 0^\circ$ . Solid line: measured. Crosses: recovered from nonredundant plane-polar NF data.

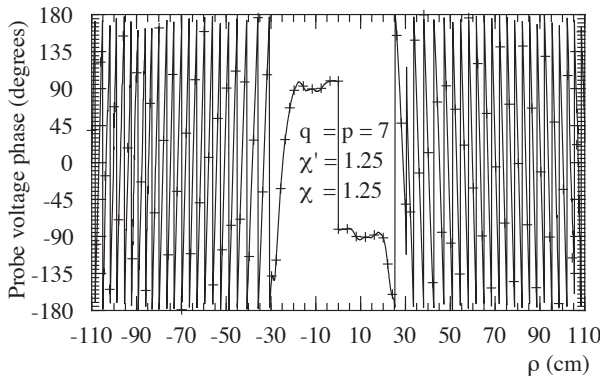


Fig. 3. Phase of  $V_\rho$  on the radial line at  $\varphi = 0^\circ$ . Solid line: measured. Crosses: recovered from nonredundant plane-polar NF data.

the principal planes E and H (Figs. 5 and 6) with those (references) obtained via a standard NF-FF cylindrical transformation.

The second set of figures refers to a H-plane monopulse antenna, placed on the plane  $z = 0$ , built by using two pyramidal horns ( $8.9 \times 6.8$  cm) at a distance of 26 cm (between centers) and a hybrid Tee, and working in the sum mode at 10 GHz. The NF data have been collected in a circle with radius 110 cm on a plane at  $z = 17$  cm, and an oblate ellipsoid with  $a = 18.3$  cm and  $b = 6.6$  cm has been adopted as AUT modelling. In Figs. 7 and 8, the amplitude and phase of  $V_\rho$  on the radial line at  $\varphi = 90^\circ$ , recovered from the nonredundant plane-polar NF data, are compared with the directly measured ones. At last, the recovered FF patterns are shown in Figs. 9 and 10. As can be seen, also for this AUT, very good NF and FF reconstructions resulted.

Finally, Table I shows the number of the NF data required by the described technique and those needed by the classical plane-polar approaches [5], [6] and by classical plane-rectangular one.

TABLE I  
NUMBER OF NF DATA NEEDED BY THE DIFFERENT NF-FF TRANSFORMATIONS

	Plane-rectangular scanning [3], [4]	Classical plane-polar approaches [5], [6]	Here described approach
AUT 1	18769	29105	2134
AUT 2	21609	33581	1675

### IV. CONCLUSION

A nonredundant NF-FF transformation with plane-polar scan using an oblate ellipsoid to shape a quasi-planar AUT has been

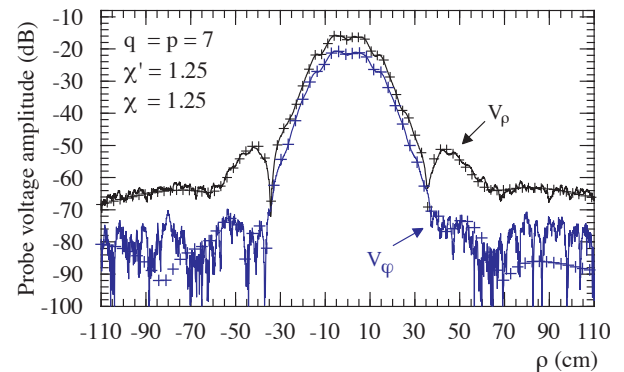


Fig. 4. Amplitudes of  $V_\rho$ ,  $V_\varphi$  on the radial line at  $\varphi = 30^\circ$ . Solid lines: measured. Crosses: recovered from nonredundant plane-polar NF data.

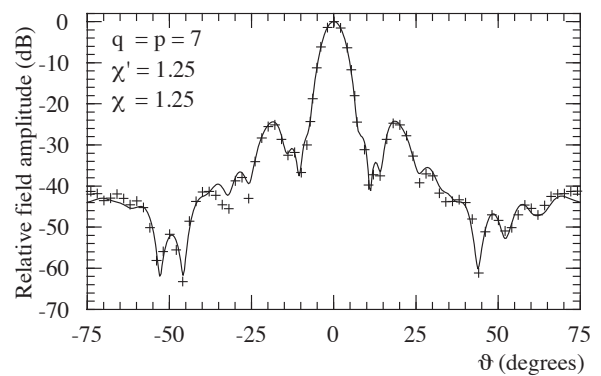


Fig. 5. E-plane pattern. Solid line: reference. Crosses: reconstructed from nonredundant plane-polar NF data.

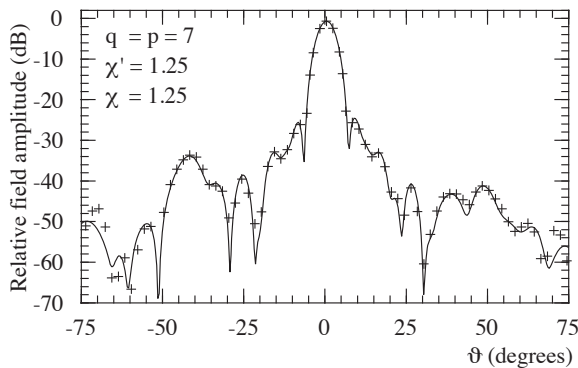


Fig. 6. H-plane pattern. Solid line: reference. Crosses: reconstructed from nonredundant plane-polar NF data.

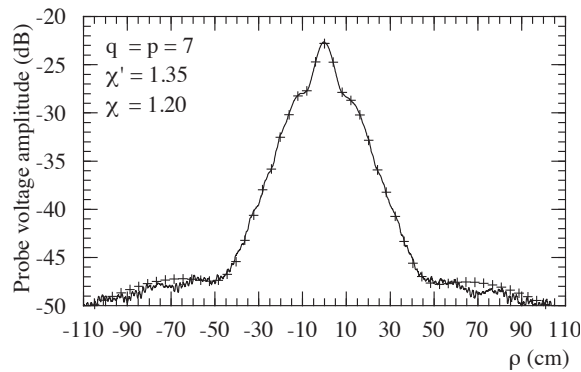


Fig. 7. Amplitude of  $V_\rho$  on the radial line at  $\phi = 90^\circ$ . Solid line: measured. Crosses: recovered from nonredundant plane-polar NF data.

experimentally tested in this letter. The very good NF and FF reconstructions obtained for two different testing antennas have confirmed the effectiveness of such a technique, which allows a remarkable measurement time saving with respect to the classical plane-rectangular and plane-polar scannings.

#### REFERENCES

- [1] A.D. Yaghjian, "An overview of near-field antenna measurements," *IEEE Trans. Antennas Propag.*, vol. AP-34, no. 1, pp. 30-45, Jan. 1986.
- [2] M.H. Francis Ed., *IEEE Recommended Practice for Near-Field Antenna Measurements*, IEEE Standard 1720-2012, Dec. 2012.
- [3] D.T. Paris, W.M. Leach, Jr., and E.B. Joy, "Basic theory of probe-compensated near-field measurements," *IEEE Trans. Antennas Propag.*, vol. AP-26, no. 3, pp. 373-379, May 1978.
- [4] E.B. Joy, W.M. Leach, Jr., G. P. Rodrigue and D.T. Paris, "Application of probe-compensated near-field measurements," *IEEE Trans. Antennas Propag.*, vol. AP-26, no. 3, pp. 379-389, May 1978.
- [5] Y. Rahmat-Samii, V. Galindo Israel, and R. Mittra, "A plane-polar approach for far-field construction from near-field measurements," *IEEE Trans. Antennas Propag.*, vol. AP-28, no. 2, pp. 216-230, March 1980.
- [6] M.S. Gatti and Y. Rahmat-Samii, "FFT applications to plane-polar near-field antenna measurements," *IEEE Trans. Antennas Propag.*, vol. 36, no. 6, pp. 781-791, June 1988.
- [7] O.M. Bucci and G. Franceschetti, "On the spatial bandwidth of scattered fields," *IEEE Trans. Antennas Propag.*, vol. AP-35, no. 12, pp. 1445-1455, Dec. 1987.
- [8] O.M. Bucci, C. Gennarelli, and C. Savarese, "Fast and accurate near-field-far-field transformation by sampling interpolation of plane-polar measurements," *IEEE Trans. Antennas Propag.*, vol. 39, no. 1, pp. 48-55, 1991.
- [9] A.D. Yaghjian, "Antenna coupling and near-field sampling in plane-polar coordinates," *IEEE Trans. Antennas Propag.*, vol. 40, no. 3, pp. 304-312, March 1992.
- [10] O.M. Bucci, C. Gennarelli, and C. Savarese, "Representation of electromagnetic fields over arbitrary surfaces by a finite and nonredundant number of samples," *IEEE Trans. Antennas Propag.*, vol. 46, no. 3, pp. 351-359, Mar. 1998.
- [11] O.M. Bucci and C. Gennarelli, "Application of nonredundant sampling representations of electromagnetic fields to NF-FF transformation techniques," *Int. J. Antennas Propag.*, vol. 2012, ID 319856, 14 pages, 2012.
- [12] O.M. Bucci, C. Gennarelli, G. Riccio, and C. Savarese, "Near-field-far-field transformation from nonredundant plane-polar data: effective modellings of the source," *IEE Proc. Microw. Antennas Propag.*, vol. 145, no. 1, pp. 33-38, Feb. 1998.
- [13] O.M. Bucci, F. D'Agostino, C. Gennarelli, G. Riccio, and C. Savarese, "NF-FF transformation with plane-polar scanning: ellipsoidal modelling of the antenna," *Automatika*, vol. 41, no. 3-4, pp. 159-164, 2000.
- [14] O.M. Bucci, G. D'Elia, and M.D. Migliore, "Advanced field interpolation from plane-polar samples: experimental verification," *IEEE Trans. Antennas Propag.*, vol. 46, no. 2, pp. 204-210, Feb. 1998.
- [15] F. D'Agostino, F. Ferrara, C. Gennarelli, R. Guerrero, and M. Migliozzi, "An effective NF-FF transformation technique with planar spiral scanning tailored for quasi-planar antennas," *IEEE Trans. Antennas Propag.*, vol. 56, no. 9, pp. 2981-2987, Sept. 2008.
- [16] A.D. Yaghjian, "Approximate formulas for the far field and gain of open-ended rectangular waveguide," *IEEE Trans. Antennas Propag.*, vol. AP-32, no. 4, pp. 378-384, April 1984.

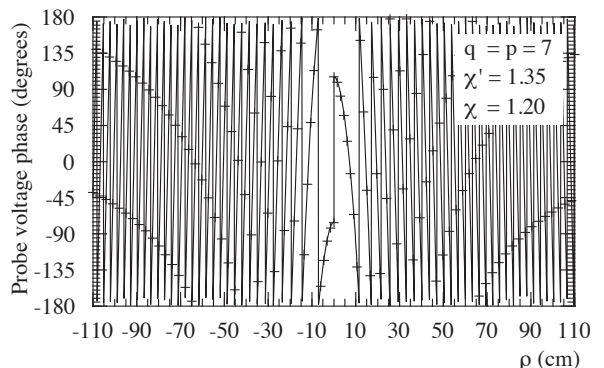


Fig. 8 . Phase of  $V_\rho$  on the radial line at  $\phi = 90^\circ$ . Solid line: measured. Crosses: recovered from nonredundant plane-polar NF data.

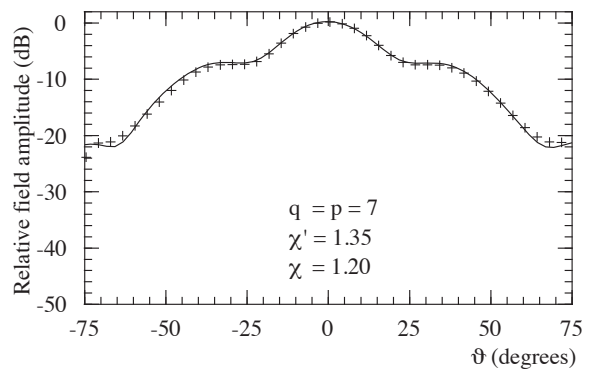


Fig. 9. E-plane pattern. Solid line: reference. Crosses: reconstructed from nonredundant plane-polar NF data.

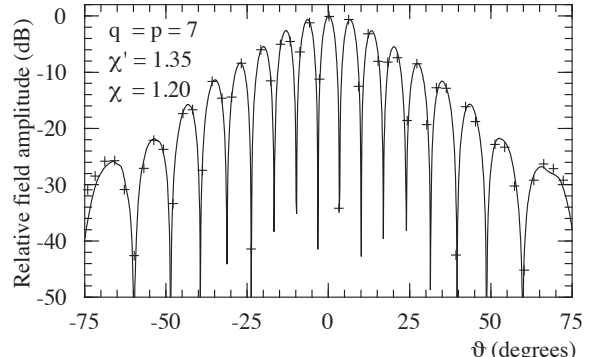


Fig. 10. H-plane pattern. Solid line: reference. Crosses: reconstructed from nonredundant plane-polar NF data.